SCIENTIFIC REPORTS

OPEN

SUBJECT AREAS:
NANOPARTICLES
NANOPHOTONICS AND PLASMONICS

Received
28 October 2014

Accepted
19 January 2015

Published
12 February 2015

Correspondence and requests for materials should be addressed to K.S. (sasaki@es.hokudai.ac.jp)

Excitation of Multipole Plasmons by Optical Vortex Beams

Kyosuke Sakai, Kensuke Nomura, Takeaki Yamamoto & Keiji Sasaki

Research Institute for Electronic Science, Hokkaido University, Sapporo, Hokkaido, 001-0020 JAPAN.

Localized surface plasmon resonance (LSPR) has been shown to exhibit a strong potential for nanoscale electromagnetic field manipulation beyond the diffraction limit. Particularly dark mode plasmons circumvent radiation loss and store the energy long in time, which raise the prospect of interesting plasmonics applications, for example biochemical sensing and nanoscale lasing. Here we theoretically investigate a method of exciting multipole plasmons, including dark modes, using normally incident light. By performing numerical calculations, we show that multipole plasmons in metal nanodisks can be selectively excited by circularly-polarized optical vortex beams. We study the electromagnetic fields of the beam cross-sections and their correspondence with the excited multipole plasmon modes with respect to spin and orbital angular momenta. The transfer of angular momentum between photons and plasmons is also discussed.

Metal nanoparticles (NPs) have been attracting widespread attention due to their unique physical and chemical properties, which originate from collective oscillations of electron density, a phenomenon known as localized surface plasmon resonance (LSPR). A variety of applications that utilize LSPR have been reported such as chemical sensors and biosensors[1,2], surface-enhanced Raman scattering[3], fluorescence enhancement[4], second harmonic generation[5], photovoltaic cells[6], and photocatalysis[7]. The optical properties of LSPR are strongly dependent on the particle size. In metal NPs that are smaller than the wavelength of light, all of the electrons experience roughly the same phase of the incident electromagnetic field, which leads to dipole plasmon resonance. As the size of the NPs increases, multipole (higher-order) plasmon modes can be excited due to phase retardation of the field inside the particle. Multipole plasmon resonances typically show lower radiative losses and higher quality factors than the dipole plasmon resonance and are hence referred to as dark mode plasmons. Applications such as plasmon lasing[8,9] and plasmon-enhanced luminescence[10] can benefit from multipole plasmons. Fano resonance is another important phenomenon that is associated with multipole plasmons[11]. Dark modes also arise from the interaction of the dipole modes in the coupled particles[12,13], but we are focusing on multipole plasmons of individual particles hereafter.

Metal NPs that inherently support multipole plasmons in a controlled manner are typically fabricated by electron beam lithography. However, in lithographically fabricated planar nanostructures such as nanodisks or nanorings, only the dipole plasmon resonance is excited by the plane wave at normal incidence, e.g. for epi-illumination in standard optical microscopy. Several studies have reported that applying an oblique incident beam or breaking the symmetry of the NPs allows multipole plasmons to be excited; however, the intensity of an excited multipole resonance is weaker than that of the simultaneously excited dipole resonance[14–16]. It is therefore important to realize an efficient scheme to excite multipole plasmon resonances selectively.

Here, we present a novel method that allows the selective and exclusive excitation of multipole plasmons of NPs. We theoretically demonstrate that a normally incident optical vortex beam with a specific azimuthal mode can excite multipole plasmons. Laguerre-Gaussian (LG) modes are employed as optical vortex beams, because they form a complete orthonormal basis set for paraxial light beams in cylindrical coordinates and thus facilitate systematic understanding. We use a gold nanodisk as a plasmonic NP, and excite LSPRs using tightly focused circularly polarized vortex beams (CPVBs). The electromagnetic field at the focus of a specific input beam shows a distinctive distribution around the beam axis that provides a good match with the corresponding plasmon resonance. The incident beams used here can be classified by the orbital and spin angular momenta of the photons. We also discuss the transfer of angular momentum from the incident vortex beam to the resultant plasmon resonance, where the total angular momentum plays a key role in the plasmonic system under investigation.

Results

Framework of numerical calculation. Before describing our numerical results, we briefly summarize the technical background. We denote the vortex beams as LG^{l}_{p}, where l is the azimuthal mode index and p is the radial mode index, giving rise to an orbital angular momentum (OAM) of $l\hbar$ per photon ($l = 0, \pm1, \pm2\ldots$)[17].Here we confine our discussion to $p = 0$, that is, a single-ringed beam. Circularly polarized beams also possess a spin angular momentum (SAM) of $\sigma\hbar$ per photon, where σ is the handedness of the circular polarization ($\sigma = \pm1$). We note that because LG modes form a complete orthonormal basis set for paraxial light beams in cylindrical coordinates, any cylindrical beam may be represented as a sum of CPVBs with appropriate weight. For example, a linearly polarized vortex beam with an OAM of $l = 1$ is given by the sum of CPVBs with ($l = 1$, $\sigma = 1$) and ($l = 1$, $\sigma = -1$). In addition, a radially polarized beam, which is known to have interesting features at the focus[18,19], can be described by the sum of CPVBs with ($l = 1$, $\sigma = -1$) and ($l = -1$, $\sigma = 1$). Therefore, the interaction between the cylindrical beams and the plasmonic nanodisk can also be understood by decomposition to CPVBs. Our notation for angular momentum, for example ($l = 1$, $\sigma = -1$), is simplified hereafter as (1,−1).

In order to investigate the plasmon resonances excited by CPVBs, we numerically calculated the electromagnetic field in the system using the finite-element method in COMSOL Multiphysics. Figure 1 shows our calculation model, which consists of a gold nanodisk (with a diameter of 400 nm and a thickness of 30 nm) suspended in air that is surrounded by a perfectly matched layer (PML) on the side and lower boundaries. The optical constant of gold was taken from Johnson and Christy[20]. We set the electric field of the focused incident beam at the upper surface. The focused excitation beam starts to propagate downwards, forming a beam waist inside the structure. We note that the beam axis penetrates the center of the nanodisk, perpendicular to the upper surface.

Figure 2 shows the instantaneous electric-field distribution (a snap shot in time) in the focus cross-section of incident CPVBs with different angular momenta (l, σ) = (0,−1), (−1,1), (−1,−1), (−2,1), (−2,−1), and (−3, 1). There are clear differences in the distribution of the electric field vectors. It should be noted that the electric field vectors rotate in time due to the orbital and spin angular momenta.

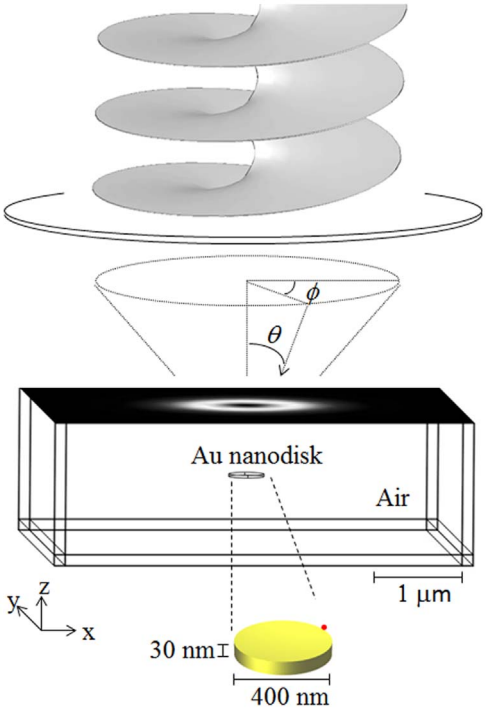

Figure 1 | Geometry of the calculation model. Red point indicates a monitor point for near-field intensity spectra.

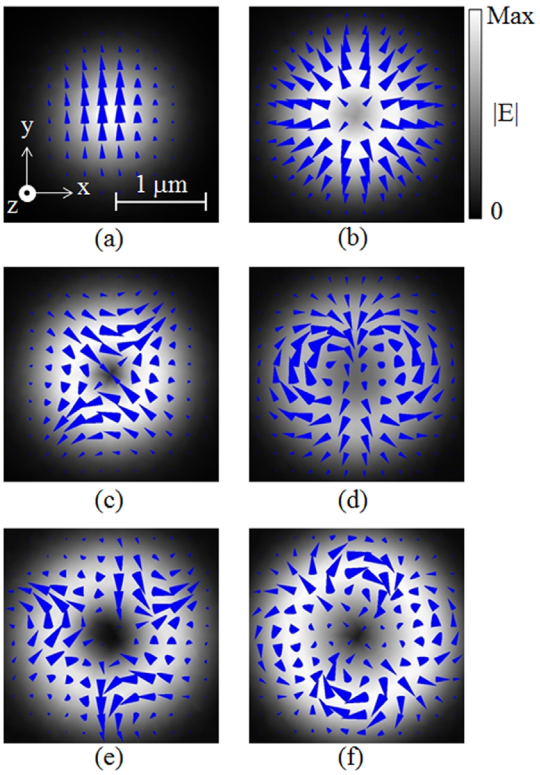

Figure 2 | Instantaneous electric-field distributions in the beam cross-section of CPVBs for (l, σ) = (a) (0, −1), (b) (−1, 1), (c) (−1, −1), (d) (−2, 1), (e) (−2, −1), and (f) (−3, 1). Blue triangles indicate the electric field vectors.

Near field spectra and field distributions of excited plasmon resonances. To discuss the excitation of plasmon resonances, we calculated the intensity spectra and distribution of the near-field around the nanodisk for beams with different angular momenta. Figure 3 shows time-averaged near-field intensity spectra obtained at a point 2 nm from the nanodisk sidewall on a horizontal plane extending from the top surface. The calculated electric-field intensity ($|E|^2$) was normalized by the field ($|E_0|^2$) obtained without the gold nanodisk. Beams with (l, σ) = (−1,1) did not show plasmon resonance, whereas those with (l, σ) = (0,−1), (−1,−1), (−2,1), (−2,−1), and (−3, 1) showed clear peaks in their spectra indicative of plasmon resonance. Beams with (l, σ) = (0,−1) and (−2,1) yielded broad spectra with a peak at ~1,250 nm. Beams with (l, σ) = (−1,−1) and (−3, 1) gave narrower spectra with a peak at 760 nm, and those with (l, σ) = (−2, −1) showed the narrowest peak, located at 630 nm.

To identify each plasmon resonance mode, we plotted the instantaneous electromagnetic-field distributions around the nanodisk at the peak wavelength (Fig. 4). The field distributions reveal the following plasmon resonance modes: dipole for (l, σ) = (0,−1), and (−2, 1); quadrupole for (l, σ) = (−1,−1), and (−3, 1); hexapole for (l, σ) = (−2,−1). When a comparison is made with the electric-field distribution of the incident beam shown in Fig. 2, it is clear that the radial component of the electric field excites plasmon resonances on the side wall of the nanodisk. For example, in the cross-section of the CPVB with (l, σ) = (−2, 1), the electric-field vectors point radially inward at twelve o'clock and radially outward at six o'clock (Fig. 2 (d)), which allows excitation of the dipole plasmon resonance. The

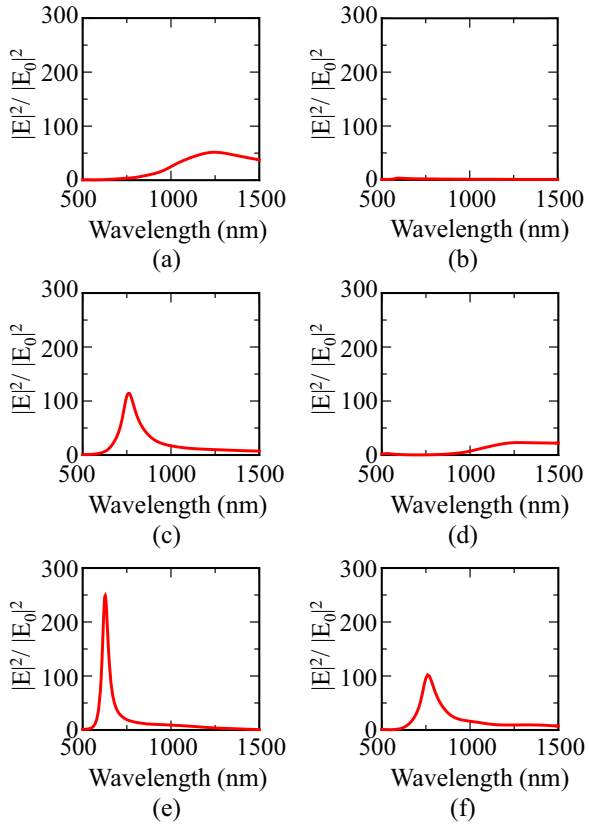

Figure 3 | Near-field intensity spectra of the nanodisk for incident CPVBs with (l, σ) = (a) (0, −1), (b) (−1, 1), (c) (−1, −1), (d) (−2, 1), (e) (−2, −1), and (f) (−3, 1).

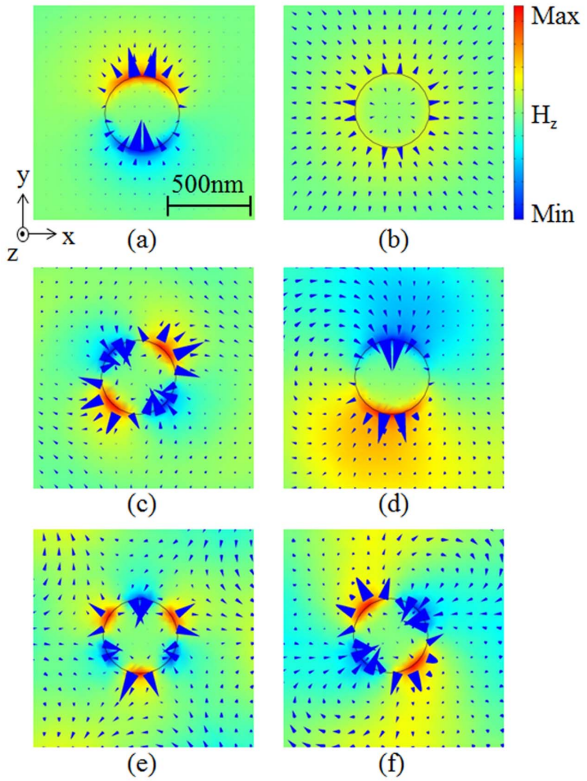

Figure 4 | Instantaneous electric-field distributions around the gold nanodisk for incident CPVBs with (l, σ) = (a) (0, −1), (b) (−1, 1), (c) (−1, −1), (d) (−2, 1), (e) (−2, −1), and (f) (−3, 1) at the peak wavelength, except for (b) at a wavelength of 600 nm. Blue triangles indicate the electric-field vectors, and color indicates the *z*-component of the magnetic field.

excited plasmon mode is exclusively dependent on the incident beam mode throughout the spectrum, even at longer wavelengths. This indicates that CPVBs can selectively excite multipole plasmons in the normal incidence configuration. The electric-field matching between the incident beam and the resultant plasmon mode influences the excitation efficiency; thus, the beam axis should coincide with the nanodisk center and the beam waist should be small enough for efficient plasmon excitation.

Discussion

We found that the excited plasmon mode is determined by the total angular momentum (TAM) transferred to the plasmon resonance in the excitation process. For a paraxial optical beam, the OAM and SAM are additive with a TAM of $J\hbar = (l + \sigma)\hbar$[17,21]. Table 1 summarizes the angular momenta of the CPVBs and the corresponding excited plasmon resonance modes. The relevant figure labels are indicated in the right-hand column. We emphasize that each value of J was obtained from two types of CPVB; for example, $J = -1$ was obtained from$(l, \sigma) = (0, -1)$ and $(-2, 1)$.The excited plasmon resonance modes were determined by the TAM (J) as follows: dipole for $|J| = 1$; quadrupole for $|J| = 2$; hexapole for $|J| = 3$. Based on the data presented in Table 1, it can be inferred that the desired plasmon resonance mode can be excited by CPVBs with a specific combination of OAM (l) and SAM (σ).

The sign of the TAM (J) determines the rotational direction of the electric-field distribution, that is, clockwise or counterclockwise with respect to the center of the nanodisk. Supplementary videos 1(a) to (f) show the dynamic evolution of the electromagnetic fields around the nanodisk for the six incident beams discussed above. Notably, the beam with $(l, \sigma) = (0, -1)$ gives rise to orbital rotational motion even though the incident beam has zero OAM ($l = 0$), whereas the beam with $(l, \sigma) = (-1, 1)$ does not show orbital rotation even with non-zero OAM ($l = -1$). We found that the orbital rotational motion originates from the TAM. These results indicate that the TAM is a key physical quantity that determines which plasmon resonance mode is excited, as well as the conserved momentum that is transferred in the process.

In conclusion, we have theoretically demonstrated that the selective excitation of multipole plasmons can be achieved using normally incident optical vortex beams. Suitable combinations of orbital and spin angular momenta produce electromagnetic fields that match the

Table 1 | Summary of angular momenta and excited plasmon resonance modes for different CPVBs

l	σ	J	Plasmon mode	Label
3	1	4	Octopole	
	−1	2	Quadrupole	
2	1	3	Hexapole	
	−1	1	Dipole	
1	1	2	Quadrupole	
	−1	0	-	
0	1	1	Dipole	
	−1	−1	Dipole	(a)
−1	1	0	-	(b)
	−1	−2	Quadrupole	(c)
−2	1	−1	Dipole	(d)
	−1	−3	Hexapole	(e)
−3	1	−2	Quadrupole	(f)
	−1	−4	Octopole	

field of a specific multipole plasmon resonance, leading to the selective and exclusive excitation of multipole plasmons. In the present plasmon-coupling system, the total angular momentum is a conserved quantity and is thus transferred from the incident beam to the excited plasmon resonance. We believe that this method for the excitation of multipole plasmons and for the transfer of angular momentum between photons and plasmons will open the way for detailed research into the control of plasmonic fields and bring associated applications a step closer. Photochemistry should benefit from the precise control of the plasmonic near-field or switching between the dipole and multipole resonances. Research fields based on optical trapping or manipulation should obtain novel tools such as nanoscale rotators.

Methods

Electric field of the focused incident beam. We analytically calculated the electric fields of tightly focused beams using the vector Debye integral, which was developed by Richards and Wolf[22], and has been used to study the vector properties of focused light[23–26]. Based on this approach, the Cartesian components of the electric-field vector ($\mathbf{e}_{(s)}$) at the focus are given in the following form:

$$\mathbf{e}_{(s)} = \begin{bmatrix} e_x{}^{(s)} \\ e_y{}^{(s)} \\ e_z{}^{(s)} \end{bmatrix} = \frac{-iA}{\pi} \int_0^{\alpha} \int_0^{2\pi} w_0(\theta) e^{ik(z_s \cos\theta + \rho_s \sin\theta \cos(\phi - \phi_s))} \mathbf{E} \sin\theta \cos^{1/2}\theta d\phi d\theta. \quad (1)$$

Here, α is the maximum focusing angle (that is, for a ray from the edge of the aperture), θ is the polar angle, ϕ is the azimuthal angle. We employ cylindrical coordinates (ρ_s, ϕ_s, z_s) at the focus. A beam mode-dependent electric-field vector $\mathbf{E}$ is given in the following form:

$$\begin{aligned} \mathbf{E} = & \left(e_r{}^{(0)} - i\sigma e_\phi{}^{(0)}\right) \begin{pmatrix} -\cos\theta\cos\phi \\ -\cos\theta\sin\phi \\ \sin\theta \end{pmatrix} \\ & + \left(e_\phi{}^{(0)} + i\sigma e_r{}^{(0)}\right) \begin{pmatrix} -\sin\phi \\ \cos\phi \\ 0 \end{pmatrix}, \end{aligned} \quad (2)$$

where $e_r{}^{(0)}$ and $e_\phi{}^{(0)}$ are given as in Ref. 26,

$$e_r{}^{(0)} = \cos([l-1]\phi), \quad e_\phi{}^{(0)} = -\sin([l-1]\phi). \quad (3)$$

We note that an apodization function $w_0(\theta)$ is given in the following form:

$$w_0(\theta) = \left(\frac{\sqrt{2}\beta_0 \sin\theta}{\sin\alpha}\right)^{|l|} L_p^{|l|}\left[2\left(\frac{\beta_0 \sin\theta}{\sin\alpha}\right)^2\right] \exp\left[-\left(\frac{\beta_0 \sin\theta}{\sin\alpha}\right)^2\right]. \quad (4)$$

Here, β_0 is the ratio of the pupil radius to the beam waist, and $L^{|l|}{}_p$ is a Laguerre polynomial given in the following form:

$$L_p^{|l|}(x) = \sum_{m=0}^{p} (-1)^m \frac{(p+l)!}{(p-m)!(l+m)!m!} x^m, \quad (5)$$

where m is an integer.

1. Mayer, K. M. & Hafner, J. H. Localized Surface Plasmon Resonance Sensors. *Chem. Rev.* **111**, 3828–3857 (2011).
2. Anker, J. N. *et al.* Bio sensing with plasmonic nanosensors. *Nat. Mater.* **7**, 442–453 (2008).
3. Stiles, P. L., Dieringer, J. A., Shah, N. C. & Van Duyne, R. P. Surface-Enhanced Raman Spectroscopy. *Annu. Rev. Anal. Chem.* **1**, 601–626 (2008).
4. Lakowicz, J. R. *et al.* Plasmon-controlled fluorescence: a new paradigm in fluorescence spectroscopy. *Analyst* **133**, 1308–1346 (2008).
5. Valev, V. K. *et al.* Asymmetric Optical Second-Harmonic Generation from Chiral G-Shaped Gold Nanostructures. *Phys. Rev. Lett.* **104**, 127401 (2010).
6. Atwater, H. A. & Polman, A. Plasmonics for improved photovoltaic devices. *Nat. Mater.* **9**, 205–213 (2010).
7. Tian, Y. & Tatsuma, T. J. Mechanisms and Applications of Plasmon-Induced Charge Separation at TiO_2 Films Loaded with Gold Nanoparticles. *J. Am. Chem. Soc.* **127**, 7632–7637 (2005).
8. Bergman, D. J. & Stockman, M. I. Surface Plasmon Amplification by Stimulated Emission of Radiation: Quantum Generation of Coherent Surface Plasmons in Nanosystems. *Phys. Rev. Lett.* **90**, 027402 (2003).
9. Noginov, M. A. *et al.* Demonstration of a spaser-based nanolaser. *Nature* **460**, 1110–1113 (2009).
10. Giannini, V. *et al.* Controlling Light Localization and Light–Matter Interactions with Nanoplasmonics. *Small* **6**, 2498–2507 (2010).
11. Luk′yanchuk, B. *et al.* The Fano resonance in plasmonic nanostructuresand metamaterials. *Nat. Mater.* **9**, 707–715 (2010).
12. Volpe, G., Cherukulappurath, S., Parramon, R. J., Molina-Terriza, G. & Quidant, R. Controlling the Optical Near Field of Nanoantennas with Spatial Phase-Shaped Beams. *Nano Lett.* **9**, 3608–3611 (2009).
13. Gómez, D. E. *et al.* The Dark Side of Plasmonics. *Nano Lett.* **13**, 3722–3728 (2013).
14. Hao, F., Larsson, E. M., Ali, T. A., Sutherland, D. S. & Nordlander, P. Shedding light on dark plasmons in gold nanorings. *Chem. Phys. Lett.* **458**, 262–266 (2008).
15. Hao, F., Nordlander, P., Sonnefraud, Y., Dorpe, P. V. & Maier, S. A. Tunability of Subradiant Dipolar and Fano-Type Plasmon Resonances in Metallic Ring/Disk Cavities: Implicationsfor Nanoscale Optical Sensing. *ACSNano* **3**, 643–652 (2009).
16. Habteyes, T. G., Dhuey, S., Cabrini, S., Schuck, P. J. & Leone, S. R. Theta-Shaped Plasmonic Nanostructures: Bringing "Dark" Multipole Plasmon Resonances into Action via Conductive Coupling. *Nano Lett.* **11**, 1819–1825 (2011).
17. Allen, L., Beijersbergen, M. W., Spreeuw, R. J. C. & Woerdman, J. P. Orbital angular momentum of light and the transformation of Laguerre-Gaussian laser modes. *Phys. Rev. A* **45**, 8185–8189 (1992).
18. Fontanta, J. R. & Pantell, R. H. A high-energy, laser accelerator for electrons using the inverse Cherenkov effect. *J. Appl. Phys.* **54**, 4285–4288 (1983).
19. Dorn, R., Quabis, S. & Leuchs, G. Sharper Focus for a Radially Polarized Light Beam. *Phys. Rev. Lett.* **91**, 233901 (2003).
20. Johnson, P. B. & Christy, R. W. Optical Constants of the Noble Metals. *Phys. Rev. B* **6**, 4370–4379 (1972).
21. Milione, G., Evans, S., Nolan, D. A. & Alfano, R. R. Higher Order Pancharatnam-Berry Phase and the Angular Momentum of Light. *Phys. Rev. Lett.* **108**, 190401 (2012).
22. Richards, B. & Wolf, E. Electromagnetic Diffraction in Optical Systems. II. Structure of the Image Field in an Aplanatic System. *Proc. R. Soc. London, Ser. A* **253**, 358–379 (1959).
23. Youngworth, K. S. & Brown, T. G. Focusing of high numerical aperture cylindrical vector Beams. *Opt. Express* **7**, 77–87 (2000).
24. Zhan, Q. & Leger, J. R. Focus shaping using cylindrical vector beams. *Opt. Express* **10**, 324–331 (2002).
25. Kozawa, Y. & Sato, S. Focusing property of a double-ring-shaped radially polarized beam. *Opt. Lett.* **31**, 820–822 (2006).
26. Kitamura, K., Sakai, K., Takayama, N., Nishimoto, M. & Noda, S. Focusing properties of vector vortex beams emitted by photonic-crystal lasers. *Opt. Lett.* **37**, 2421–2423 (2012).

Acknowledgments

The authors thank Y. Tanaka and H. Fujiwara for helpful discussions and suggestions. This work was partly supported by Grant-in-Aid for Scientific Research (A) 23246016.

Author contributions

K. Sakai and K. Sasaki conceived the idea. K. Sakai, K.N. and T.Y. performed the numerical calculations. K. Sakai wrote the manuscript. K. Sasaki supervised the project.

Additional information

Supplementary information accompanies this paper at http://www.nature.com/scientificreports

Competing financial interests: The authors declare no competing financial interests.

How to cite this article: Sakai, K., Nomura, K., Yamamoto, T. & Sasaki, K. Excitation of Multipole Plasmons by Optical Vortex Beams. *Sci. Rep.* **5**, 8431; DOI:10.1038/srep08431 (2015).